Nuclear Engineering and Design 51 (1979) 389–401

FINITE ELEMENT FORMULATION AND SOLUTION OF NONLINEAR HEAT TRANSFER

Klaus-Jürgen BATHE and Mohammad R. KHOSHGOFTAAR
Department of Mechanical Engineering, Massachusetts Institute of Technology, Cambridge, MA 02139, USA

Received 31 July 1978

A general and effective finite element formulation for analysis of nonlinear steady-state and transient heat transfer is presented. Heat conduction conditions, and convection and radiation boundary conditions are considered. The solutions of the incremental heat transfer equations is achieved using Newton–Raphson iteration, and in transient analysis using a one-step α-family time integration scheme. The stability and accuracy of the time integration is discussed. The solution techniques have been implemented, and the results of various sample solutions are discussed and evaluated.

1. Introduction

Since the advent of the electronic digital computer, the associated development of effective finite element procedures for stress analysis of structures and continua [1,2], and the application of finite element techniques to the solution of heat transfer problems [3–5], the predominant numerical method for analysis of heat transfer problems remained the finite difference method. It is only during the very recent years that the advantages of a finite element analysis have become more clear. Apart from the benefits that can be obtained from the generality of the finite element method, e.g. to approximate geometries and material properties, emphasis on the development of effective finite element procedures for field problems is also important, because the application of finite element methods shows much promise for the solution of coupled stress and field problems [6].

The objective in this paper is to present a general and effective incremental finite element formulation for analysis of nonlinear steady-state and transient heat transfer, the numerical algorithms employed for solution and various experiences that have been gained in the evaluation of the solution procedures. The analysis techniques have been implemented in the computer program ADINAT and are employed for the solution of heat transfer problems with conduction, convection and radiation conditions [7]. In this work decoupled stress and temperature conditions are assumed, but the ultimate objective is also the development of effective solution techniques for analysis of coupled stress and field problems.

2. Finite element solution of nonlinear heat transfer

The governing equations for heat transfer analysis of a body idealized by a system of finite elements can be derived by invoking the stationarity of a functional or using the Galerkin method [2]. However, the realization that, physically, heat flow equilibrium is to be satisfied at the finite element nodes (and in an integrated sense throughout the finite element idealization) yields additional insight into the solution process, and provides an effective basis for the development of the incremental heat flow equilibrium equations for linear and nonlinear steady-state and transient analysis.

2.1. Incremental field equations

As in incremental finite element stress analysis [2], assume that the conditions of the body at time t have been calculated, and that the temperatures are to be determined for time $t + \Delta t$, where Δt is the time increment. To evaluate the temperatures at time $t + \Delta t$ the heat flow equilibrium of the body is considered

at time $t + \alpha\Delta t$, where $0 \leqslant \alpha \leqslant 1$ and α is chosen to obtain optimum stability and accuracy in the solution. (In steady-state analysis $\alpha = 1$ and Δt is used to determine the heat flow increment, but is otherwise a dummy variable.) Considering heat flow equilibrium at time $t + \alpha\Delta t$ the basic equation to be satisfied for a three-dimensional body is

$$\int_V \delta\boldsymbol{\theta}'^T\, {}^{t+\alpha\Delta t}\mathbf{k}\, {}^{t+\alpha\Delta t}\boldsymbol{\theta}'\, \mathrm{d}V = {}^{t+\alpha\Delta t}Q + \int_{S_c} \delta\theta^S\, {}^{t+\alpha\Delta t}h({}^{t+\alpha\Delta t}\theta_e - {}^{t+\alpha\Delta t}\theta^S)\, \mathrm{d}S + \int_{S_r} \delta\theta^S\, {}^{t+\alpha\Delta t}\kappa({}^{t+\alpha\Delta t}\theta_r - {}^{t+\alpha\Delta t}\theta^S)\, \mathrm{d}S \qquad (1)$$

where θ is the temperature of the body, θ^S is the surface temperature, θ_e is the environmental temperature, θ_r is the temperature of a radiating source and the superscript $t + \alpha\Delta t$ denotes "at time $t + \alpha\Delta t$". Also, δ denotes "variation in", h is the surface convection coefficient, κ is a radiation coefficient and

$$\boldsymbol{\theta}'^T = \begin{bmatrix} \frac{\partial\theta}{\partial x} & \frac{\partial\theta}{\partial y} & \frac{\partial\theta}{\partial z} \end{bmatrix},$$

$$\mathbf{k} = \begin{bmatrix} k_x & 0 & 0 \\ 0 & k_y & 0 \\ 0 & 0 & k_z \end{bmatrix},$$

where k_x, k_y and k_z are the thermal conductivities corresponding to the principal directions of conductivity x, y and z.

In eq. (1) S_c and S_r are the surface areas with convection and radiation boundary conditions respectively, and ${}^{t+\alpha\Delta t}Q$ is the virtual work of the external heat flow input to the system at time $t + \alpha\Delta t$. The quantity ${}^{t+\alpha\Delta t}Q$ includes the effects of surface heat flow inputs, q^S, (that are not included in the convection and radiation boundary conditions), internal heat generation, $\tilde{q}^B$, and temperature-dependent heat capacity, c. Hence

$${}^{t+\alpha\Delta t}Q = \int_S \delta\theta^S\, {}^{t+\alpha\Delta t}q^S\, \mathrm{d}S + \int_V \delta\theta({}^{t+\alpha\Delta t}\tilde{q}^B - {}^{t+\alpha\Delta t}c\, {}^{t+\alpha\Delta t}\dot{\theta})\, \mathrm{d}V \qquad (2)$$

It should be noted that in linear analysis ${}^{t+\alpha\Delta t}\mathbf{k}$, ${}^{t+\alpha\Delta t}c$ and ${}^{t+\alpha\Delta t}h$ are constant and radiation boundary conditions are not included. Hence eq. (1) can be solved directly for the temperature ${}^{t+\alpha\Delta t}\theta$, see eq. (9). However, in nonlinear analysis eq. (1) is a nonlinear equation for the temperature at time $t + \alpha\Delta t$. Using eq. (2) for steady-state analysis or transient analysis with implicit time integration { explicit time integration (case $\alpha = 0$) is performed as in linear analysis [2] } the solution is obtained effectively by linearizing eq. (1) as shown in table 1 and then using the modified Newton–Raphson iteration method. In this

Table 1
Linearization of nonlinear heat flow equilibrium equations

1. Equilibrium equations at time $t + \alpha\Delta t$

$$\int_V \delta\boldsymbol{\theta}'^T\, {}^{t+\alpha\Delta t}\mathbf{k}\, {}^{t+\alpha\Delta t}\boldsymbol{\theta}'\, \mathrm{d}V = {}^{t+\alpha\Delta t}Q + \int_{S_c} \delta\theta^S\, {}^{t+\alpha\Delta t}h({}^{t+\alpha\Delta t}\theta_e - {}^{t+\alpha\Delta t}\theta^S)\, \mathrm{d}S + \int_{S_r} \delta\theta^S\, {}^{t+\alpha\Delta t}\kappa({}^{t+\alpha\Delta t}\theta_r - {}^{t+\alpha\Delta t}\theta^S)\, \mathrm{d}S$$

2. Linearization of equations
We use:

$${}^{t+\alpha\Delta t}\theta = {}^t\theta + \theta\,;\quad {}^{t+\alpha\Delta t}\boldsymbol{\theta}' = {}^t\boldsymbol{\theta}' + \boldsymbol{\theta}'\,;\quad {}^{t+\alpha\Delta t}\mathbf{k} = {}^t\mathbf{k} + \mathbf{k}\,;$$

$${}^{t+\alpha\Delta t}h = {}^th + h\,;\quad {}^{t+\alpha\Delta t}\kappa = {}^t\kappa + \kappa$$

and assume:

$${}^{t+\alpha\Delta t}\mathbf{k}\, {}^{t+\alpha\Delta t}\boldsymbol{\theta}' = {}^t\mathbf{k}({}^t\boldsymbol{\theta}' + \boldsymbol{\theta}')\,;$$

$${}^{t+\alpha\Delta t}h({}^{t+\alpha\Delta t}\theta_e - {}^{t+\alpha\Delta t}\theta^S) = {}^th({}^{t+\alpha\Delta t}\theta_e - {}^t\theta^S - \theta^S)$$

$${}^{t+\alpha\Delta t}\kappa({}^{t+\alpha\Delta t}\theta_r - {}^{t+\alpha\Delta t}\theta^S) = {}^t\kappa({}^{t+\alpha\Delta t}\theta_r - {}^t\theta^S - \theta^S)$$

Substituting into the equations of heat flow equilibrium we obtain

$$\int_V \delta\boldsymbol{\theta}'^T\, {}^t\mathbf{k}\boldsymbol{\theta}'\, \mathrm{d}V + \int_{S_c} \delta\theta^S\, {}^th\, \theta^S\, \mathrm{d}S + \int_{S_r} \delta\theta^S\, {}^t\kappa\, \theta^S\, \mathrm{d}S = {}^{t+\alpha\Delta t}Q + \int_{S_c} \delta\theta^S\, {}^th({}^{t+\alpha\Delta t}\theta_e - {}^t\theta^S)\, \mathrm{d}S + \int_{S_r} \delta\theta^S\, {}^t\kappa({}^{t+\alpha\Delta t}\theta_r - {}^t\theta^S)\, \mathrm{d}S - \int_V \delta\boldsymbol{\theta}'^T\, {}^t\mathbf{k}\, {}^t\boldsymbol{\theta}'\, \mathrm{d}V$$

iteration we solve, for $i = 1, 2, \ldots$,

$$\int_V \delta\boldsymbol{\theta}'^T\, {}^t\mathbf{k}\, \Delta\boldsymbol{\theta}'^{(i)}\, dV + \int_{S_c} \delta\theta^S\, {}^t h\, \Delta\theta^{S(i)}\, dS + \int_{S_r} \delta\theta^S\, {}^t\kappa\, \Delta\theta^{S(i)}\, dS = {}^{t+\alpha\Delta t}Q + \int_{S_c} \delta\theta^S\, {}^{t+\alpha\Delta t}h^{(i-1)}({}^{t+\alpha\Delta t}\theta_e - {}^{t+\alpha\Delta t}\theta^{S(i-1)})\, dS + \int_{S_r} \delta\theta^S\, {}^{t+\alpha\Delta t}\kappa^{(i-1)}({}^{t+\alpha\Delta t}\theta_r - {}^{t+\alpha\Delta t}\theta^{S(i-1)})\, dS - \int_V \delta\boldsymbol{\theta}'^T\, {}^{t+\alpha\Delta t}\mathbf{k}^{(i-1)}\, {}^{t+\alpha\Delta t}\boldsymbol{\theta}'^{(i-1)}\, dV, \quad (3)$$

where

$${}^{t+\alpha\Delta t}\theta^{(i)} = {}^{t+\alpha\Delta t}\theta^{(i-1)} + \Delta\theta^{(i)}, \quad (4)$$

and ${}^{t+\alpha\Delta t}h^{(i-1)}$, ${}^{t+\alpha\Delta t}\kappa^{(i-1)}$, and ${}^{t+\alpha\Delta t}\mathbf{k}^{(i-1)}$ are the convection and radiation coefficients and the conductivity matrix that correspond to the temperature ${}^{t+\alpha\Delta t}\theta^{(i-1)}$.

In transient analysis ${}^{t+\alpha\Delta t}Q$ is a function of ${}^{t+\alpha\Delta t}\dot{\theta}$, which is approximated using a time integration scheme as discussed in section 2.4.

2.2. Finite element discretization

It is effective to employ isoparametric finite element discretization, in which we use for an element [2]:

$$x = \sum_{i=1}^{N} h_i x_i; \quad y = \sum_{i=1}^{N} h_i y_i; \quad z = \sum_{i=1}^{N} h_i z_i, \quad (5)$$

and

$${}^{t+\alpha\Delta t}\theta = \sum_{i=1}^{N} h_i\, {}^{t+\alpha\Delta t}\theta_i; \quad {}^t\theta = \sum_{i=1}^{N} h_i\, {}^t\theta_i, \quad \Delta\theta = \sum_{i=1}^{N} h_i\, \Delta\theta_i, \quad (6)$$

where the h_i are the element interpolation functions; N is the number of nodal points; x_i, y_i, z_i are the coordinates of nodal point i, and ${}^{t+\alpha\Delta t}\theta_i$, ${}^t\theta_i$, $\Delta\theta_i$ are the temperatures at times $t+\alpha\Delta t$, t and temperature increment at nodal point i. Eq. (5) has been written for a three-dimensional element; for a one- or two-dimensional element only the appropriate coordinate interpolations would be employed.

The finite element incremental heat flow equilibrium equations are derived by substituting the interpolations of eqs. (5) and (6) into eqs. (2) and (3). As usual, only a single finite element is considered, because the equilibrium equations of the complete system of finite elements are obtained by assemblage of the individual finite element matrices [2]. Table 2 summarizes the finite element matrices that are obtained from eqs. (2) and (3), when the interpolations in eqs. (5) and (6) are substituted. Using the results of table 2, eqs. (2) and (3) are thus for a single finite element:

$$({}^t\mathbf{K}^k + {}^t\mathbf{K}^c + {}^t\mathbf{K}^r)\, \Delta\boldsymbol{\theta}^{(i)} = {}^{t+\alpha\Delta t}\mathbf{Q} + {}^{t+\alpha\Delta t}\mathbf{Q}^{c(i-1)} + {}^{t+\alpha\Delta t}\mathbf{Q}^{r(i-1)} - {}^{t+\alpha\Delta t}\mathbf{Q}^{k(i-1)}, \quad (7)$$

where

$${}^{t+\alpha\Delta t}\boldsymbol{\theta}^{(i)} = {}^{t+\alpha\Delta t}\boldsymbol{\theta}^{(i-1)} + \Delta\boldsymbol{\theta}^{(i)}. \quad (8)$$

Considering table 2 it should be noted that the temperature interpolation matrices, $\mathbf{H}$ and $\mathbf{H}^S$, are directly constructed from the element interpolation functions, and the temperature gradient interpolation matrices, $\mathbf{B}$, are obtained from the derivatives of the interpolation functions as described in [2,p. 187].

Eq. (7) is the general incremental heat flow equilibrium equation, that is valid for linear and nonlinear analysis. However, in linear analysis, the equation can be used in a more effective form. Namely, if the conductivity, specific heat and convection coefficients are constant, i.e. ${}^t\mathbf{K}^k$ and ${}^t\mathbf{K}^c$ are constant matrices, and radiation boundary conditions are not included, eq. (7) becomes:

$$(\mathbf{K}^k + \mathbf{K}^c)\, {}^{t+\alpha\Delta t}\boldsymbol{\theta} = {}^{t+\alpha\Delta t}\mathbf{Q} + {}^{t+\alpha\Delta t}\mathbf{Q}^e \quad (9)$$

where $\mathbf{K}^c$ and ${}^{t+\alpha\Delta t}\mathbf{Q}^e$ are defined in table 2.

2.3. Incorporation of boundary conditions

Convection and radiation boundary conditions are taken into account by including the matrices ${}^t\mathbf{K}^c$ and ${}^t\mathbf{K}^r$ and the vectors ${}^{t+\alpha\Delta t}\mathbf{Q}^c$ and ${}^{t+\alpha\Delta t}\mathbf{Q}^r$ in the heat flow equilibrium equations, eq. (7). Additional external heat flow input on the boundary is specified in ${}^{t+\alpha\Delta t}\mathbf{Q}$ as surface heat flow input (see table 2).

Table 2
Finite element matrices

Integral	Finite element evaluation
$\int_V \delta\boldsymbol{\theta}'^T\, {}^t\mathbf{k}\, \Delta\boldsymbol{\theta}'^{(i)}\, dV$	${}^t\mathbf{K}^k\, \Delta\boldsymbol{\theta}^{(i)} = (\int_V \mathbf{B}^T\, {}^t\mathbf{k}\, \mathbf{B}\, dV)\, \Delta\boldsymbol{\theta}^{(i)}$
$\int_{S_c} \delta\theta^S\, {}^t h\, \Delta\theta^{S(i)}\, dS$	${}^t\mathbf{K}^c\, \Delta\boldsymbol{\theta}^{(i)} = (\int_{S_c} {}^t h\, \mathbf{H}^{ST}\mathbf{H}^S\, dS)\, \Delta\boldsymbol{\theta}^{(i)}$
$\int_{S_r} \delta\theta^S\, {}^t\kappa\, \Delta\theta^{S(i)}\, dS$	${}^t\mathbf{K}^r\, \Delta\boldsymbol{\theta}^{(i)} = (\int_{S_r} {}^t\kappa\, \mathbf{H}^{ST}\mathbf{H}^S\, dS)\, \Delta\boldsymbol{\theta}^{(i)}$
${}^{t+\alpha\Delta t}\tilde{Q}$ [in eq. (2)]	${}^{t+\alpha\Delta t}\mathbf{Q}^{(i-1)} = {}^{t+\alpha\Delta t}\tilde{\mathbf{Q}} - {}^{t+\alpha\Delta t}\mathbf{C}^{(i-1)}\, {}^{t+\alpha\Delta t}\dot{\boldsymbol{\theta}}^{(i-1)}$
	${}^{t+\alpha\Delta t}\tilde{\mathbf{Q}} = \int_V \mathbf{H}^T\, {}^{t+\alpha\Delta t}\tilde{q}^B\, dV + \int_S \mathbf{H}^{ST}\, {}^{t+\alpha\Delta t}q^S\, dS$
	${}^{t+\alpha\Delta t}\mathbf{C}^{(i-1)} = \int_V {}^{t+\alpha\Delta t}c^{(i-1)}\, \mathbf{H}^T\mathbf{H}\, dV$
$\int_{S_c} \delta\theta^S\, {}^{t+\alpha\Delta t}h^{(i-1)}({}^{t+\alpha\Delta t}\theta_e - {}^{t+\alpha\Delta t}\theta^{S(i-1)})\, dS$	${}^{t+\alpha\Delta t}\mathbf{Q}^{c(i-1)} = \int_{S_c} {}^{t+\alpha\Delta t}h^{(i-1)}\, \mathbf{H}^{ST}[\mathbf{H}^S({}^{t+\alpha\Delta t}\boldsymbol{\theta}_e - {}^{t+\alpha\Delta t}\boldsymbol{\theta}^{(i-1)})]\, dS$
$\int_{S_r} \delta\theta^S\, {}^{t+\alpha\Delta t}\kappa^{(i-1)}({}^{t+\alpha\Delta t}\theta_r - {}^{t+\alpha\Delta t}\theta^{S(i-1)})\, dS$	${}^{t+\alpha\Delta t}\mathbf{Q}^{r(i-1)} = \int_{S_r} {}^{t+\alpha\Delta t}\kappa^{(i-1)}\, \mathbf{H}^{ST}[\mathbf{H}^S({}^{t+\alpha\Delta t}\boldsymbol{\theta}_r - {}^{t+\alpha\Delta t}\boldsymbol{\theta}^{(i-1)})]\, dS$
$\int_V \delta\boldsymbol{\theta}'^T\, {}^{t+\alpha\Delta t}\mathbf{k}^{(i-1)}\, {}^{t+\alpha\Delta t}\boldsymbol{\theta}'^{(i-1)}\, dV$	${}^{t+\alpha\Delta t}\mathbf{Q}^{k(i-1)} = \int_V \mathbf{B}^T[{}^{t+\alpha\Delta t}\mathbf{k}^{(i-1)}\mathbf{B}\, {}^{t+\alpha\Delta t}\boldsymbol{\theta}^{(i-1)}]\, dV$
$\int_{S_c} h\, \delta\theta^S\, {}^{t+\alpha\Delta t}\theta^S\, dS$	$\mathbf{K}^c\, {}^{t+\alpha\Delta t}\boldsymbol{\theta} = (\int_{S_c} h\, \mathbf{H}^{ST}\mathbf{H}^S\, dS)\, {}^{t+\alpha\Delta t}\boldsymbol{\theta}$
$\int_{S_c} h\, \delta\theta^S\, {}^{t+\alpha\Delta t}\theta_e\, dS$	${}^{t+\alpha\Delta t}\mathbf{Q}^e = \int_{S_c} h\, \mathbf{H}^{ST}[\mathbf{H}^S\, {}^{t+\alpha\Delta t}\boldsymbol{\theta}_e]\, dS$

The only boundary conditions that have not yet been taken into account in eq. (7) are temperature boundary conditions. Zero temperature conditions at a nodal point are simply imposed by not including the heat flow equilibrium equation corresponding to that nodal point. In order to specify a nonzero temperature condition, it is effective to employ the procedure that is used to impose convection boundary conditions. Namely, by specifying a large value of h the surface temperature will be equal to the applied temperature.

2.4. Step-by-step time integration

Considering the finite element heat transfer equilibrium equations, we recognize that for any time t these equations can be written in the form,

$$\mathbf{C}\dot{\boldsymbol{\theta}} + \mathbf{K}\boldsymbol{\theta} = \bar{\mathbf{Q}}\,, \tag{10}$$

where $\mathbf{C}$ is the heat capacity matrix, $\bar{\mathbf{Q}}$ is a vector of thermal nodal loads and

$$\mathbf{K} = \mathbf{K}^k + \mathbf{K}^c + \mathbf{K}^r\,. \tag{11}$$

In eq. (10) the matrices $\mathbf{C}$ and $\mathbf{K}$ and the vector $\bar{\mathbf{Q}}$ are in general temperature dependent.

2.4.1. Time integration schemes

For transient analysis it is effective to employ numerical time integration [2]. In this study we consider a family of one-step methods with the following assumptions [8–10]:

$$^{t+\alpha\Delta t}\dot{\boldsymbol{\theta}} = (^{t+\Delta t}\boldsymbol{\theta} - {}^{t}\boldsymbol{\theta})/\Delta t\,, \tag{12}$$

and

$$^{t+\alpha\Delta t}\boldsymbol{\theta} = (1-\alpha)\,{}^{t}\boldsymbol{\theta} + \alpha\,{}^{t+\Delta t}\boldsymbol{\theta}\,. \tag{13}$$

Using eq. (10) at time $t+\alpha\Delta t$ [as was done in the formulation, eq. (7)], and the assumptions in eq. (12) and (13) we obtain for an effective incremental solution the equations corresponding to an Euler formula with time step $\alpha\Delta t$,

$$a_0\,{}^{t+\alpha\Delta t}\mathbf{C}\,{}^{t+\Delta t/a_1}\boldsymbol{\theta} + {}^{t+\alpha\Delta t}\mathbf{K}\,{}^{t+\alpha\Delta t}\boldsymbol{\theta} = {}^{t+\alpha\Delta t}\bar{\mathbf{Q}} + a_0\,{}^{t+\alpha\Delta t}\mathbf{C}\,{}^{t}\boldsymbol{\theta}\,, \tag{14}$$

and also

$$^{t+\Delta t}\boldsymbol{\theta} = a_1\,{}^{t+\Delta t/a_1}\boldsymbol{\theta} + (1-a_1)\,{}^{t}\boldsymbol{\theta}\,, \tag{15}$$

where

$$a_0 = (\Delta t)^{-1}\,,\ a_1 = 1 \text{ for } \alpha = 0\,,$$

$$a_0 = (\alpha\Delta t)^{-1}\,,\ a_1 = \alpha^{-1} \text{ for } \alpha \neq 0\,.$$

In the above scheme we have the Euler forward method when $\alpha = 0$ and the Euler backward method when $\alpha = 1$ [2].

Since, in nonlinear analysis, $^{t+\alpha\Delta t}\dot{\boldsymbol{\theta}}$ must be calculated by an iterative technique, we employ for the assemblage of elements:

$$^{t+\alpha\Delta t}\dot{\boldsymbol{\theta}}^{(i)} = (^{t+\alpha\Delta t}\boldsymbol{\theta}^{(i-1)} + \Delta\boldsymbol{\theta}^{(i)} - {}^{t}\boldsymbol{\theta})/(\alpha\Delta t)\,. \tag{16}$$

This relation is obtained from eqs. (12) and (13) by eliminating $^{t+\Delta t}\boldsymbol{\theta}$ and then using eq. (8).

2.4.2. Stability and accuracy

The stability of the time integration scheme is analyzed as usual by considering the single degree-of-freedom nonlinear heat transfer equation

$$\dot{\theta} + \lambda(\theta, t)\,\theta = 0\,, \tag{17}$$

where it is assumed that the effect of temperature dependent loads is negligible. Using the integration scheme we obtain:

$$^{t+\Delta t}\theta = \left[\frac{1-(1-\alpha)\,\Delta t\,{}^{t+\alpha\Delta t}\lambda}{1+\alpha\Delta t\,{}^{t+\alpha\Delta t}\lambda}\right] {}^{t}\theta \tag{18}$$

where for stability:

$$\left|\frac{1-(1-\alpha)\,\Delta t\,{}^{t+\alpha\Delta t}\lambda}{1+\alpha\Delta t\,{}^{t+\alpha\Delta t}\lambda}\right| \leqslant 1\,. \tag{19}$$

Here, it should be noted that λ contains the effects of conduction, convection and radiation, because the convection and radiation matrices are in eq. (10) simply added to the conduction matrix. From eq. (19) we obtain the following results:

(i) for $\alpha \geqslant \frac{1}{2}$ the scheme is unconditionally stable;

(ii) for $\alpha < \frac{1}{2}$ the scheme is stable provided $\Delta t \leqslant 2/[(1-2\alpha)\,{}^{t+\alpha\Delta t}\lambda]$.

The solution accuracy of the scheme is also analyzed considering eq. (17). Of particular interest are the Euler forward method ($\alpha = 0$), the trapezoidal rule ($\alpha = \frac{1}{2}$) and the Euler backward method ($\alpha = 1$). To identify the accuracy of the Euler forward method we employ the Taylor series expansion

$$^{t+\Delta t}\theta = {}^{t}\theta + \Delta t\,{}^{t}\dot{\theta} + \frac{\Delta t^2}{2!}\,{}^{t}\ddot{\theta} + \frac{\Delta t^3}{3!}\,{}^{t}\dddot{\theta} + \ldots\,, \tag{20}$$

and obtain by rearranging:

$$^{t}\dot{\theta} = (^{t+\Delta t}\theta - {}^{t}\theta)/\Delta t - \frac{\Delta t}{2!}\,{}^{t}\ddot{\theta} - \frac{\Delta t^2}{3!}\,{}^{t}\dddot{\theta} - \ldots\,. \tag{21}$$

Similarly, to identify the accuracy of the Euler backward method, we can obtain

$$^{t+\Delta t}\dot{\theta} = (^{t+\Delta t}\theta - {}^{t}\theta)/\Delta t + \frac{\Delta t}{2!}\,{}^{t+\Delta t}\ddot{\theta} - \frac{\Delta t^2}{3!}\,{}^{t+\Delta t}\dddot{\theta} + - \ldots\,. \tag{22}$$

Eqs. (21) and (22) show that both Euler methods are first-order accurate. However, in the Euler backward method the terms that are truncated to represent the time derivative approximately [compare eqs. (12) and (22)] alternate in sign, which can result in significantly better solution accuracy using this method.

To identify the accuracy of the trapezoidal rule we recognize that the total solution for $^{t+\Delta t}\theta$ involves a backward Euler step and then a forward Euler step each with time step $\Delta t/2$. Thus, using backward and forward Taylor series expansions about $t + \Delta t/2$ for $^{t}\theta$ and $^{t+\Delta t}\theta$, respectively, we obtain using eq. (17)

at time $t + \Delta t/2$:

$$
{}^{t+\Delta t}\theta = \frac{1 - \Delta t/2\ {}^{t+\Delta t/2}\lambda}{1 + \Delta t/2\ {}^{t+\Delta t/2}\lambda}\ {}^{t}\theta
+ \left(\frac{\Delta t}{2}\right)^2 \frac{1}{2!} \frac{\Delta t\ {}^{t+\Delta t/2}\lambda}{1 + \Delta t/2\ {}^{t+\Delta t/2}\lambda}\ {}^{t+\Delta t/2}\ddot{\theta}
+ \left(\frac{\Delta t}{2}\right)^3 \frac{1}{3!} \frac{2}{1 + \Delta t/2\ {}^{t+\Delta t/2}\lambda}\ {}^{t+\Delta t/2}\dddot{\theta} + \ldots . \quad (23)
$$

Thus, the integration scheme is second order accurate for $\alpha = \frac{1}{2}$.

In comparing the Euler forward, Euler backward and trapezoidal methods the following considerations need also be included. Using the Euler forward method, experience shows that the time step to be employed for an accurate solution may still be significantly smaller than the critical time step for stability. Considering the Euler backward method the predicted response using this method converges monotonically to the exact solution as Δt is decreased, and shows no noise effect [see eq. (18)] whereas the trapezoidal integration scheme produces response oscillation for Δt larger than $2/{}^{t+\Delta t/2}\lambda$ [9]. This effect is displayed in the analysis of a solid cylinder with radiation boundary conditions in section 4. However, the results also show that using a larger time step Δt the solution with the Euler backward method predicts the response more accurately than the solution with the trapezoidal rule.

2.4.3. Convergence of iteration

The stability and accuracy analysis, and the incremental formulation in section 2 assume that the modified Newton iteration converges. This convergence is guaranteed in transient analysis provided the time step Δt is small enough, and in steady-state analysis provided the increase in the conductivity or of the convection, radiation coefficients within the incremental step is not too large.

3. Analogies to other field problems

Considering the heat transfer governing equations it is noted that the same equations are also applicable to the analysis of other field problems provided the appropriate variables are employed. The equations are, for example, applicable to problems of flow in porous media, torsion, incompressible and irrotational flow, electrostatic field analysis and so on, as summarized in [7,11–13]. In practice the analogies mean that a heat transfer analysis computer program can also directly be employed for the solution of these analogous field problems [7,14,15].

4. Sample solutions

In this section the results of a number of sample analyses are given using the formulations and numerical algorithms presented above. The problem solutions have been obtained with the computer program ADINAT in which one, two and three-dimensional variable-number-node elements have been implemented [2,7]. The objective in these analyses was to identify numerically to some degree the stability and accuracy characteristics of the solution techniques. In the transient analyses, the time steps were selected such that the maximum nodal point temperature change during a time step was about 10% (or less) of the last calculated nodal point temperatures.

4.1. Nonlinear steady-state temperature analysis of a slab with internal heat generation

An infinitely long slab, $2L$ thick, with constant surface temperature θ^S and constant internal heat generation $\tilde{q}^B$ was analyzed. Fig. 1 shows the finite element idealization employed in the analysis. Because of symmetry conditions, only one half of the slab was considered. The thermal conductivity k was assumed to vary linearly with temperature as follows:

$$k = k_S(1 + \beta\theta)$$

k_S = conductivity at θ^S

For the finite element model, ten equally spaced one-dimensional heat flow elements were used to model one half of the thickness of the slab. For various values of β, the steady-state temperature distributions were obtained using ADINAT.

The ADINAT solution is compared in fig. 2 with an analytical solution [16], and good correspondence is observed. In the nonlinear solution 6 to 9 equilibrium iterations were used to converge to tol = 10^{-4} (see table 3).

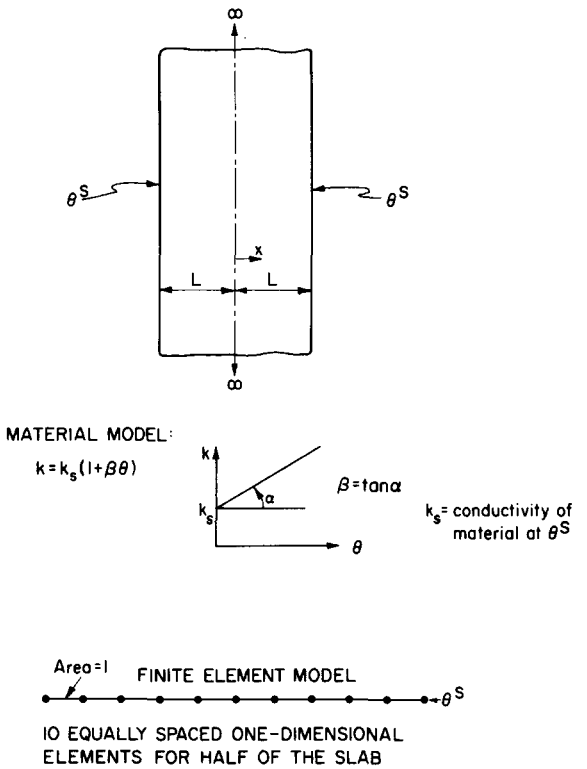

Fig. 1. Nonlinear temperature analysis of slab with internal heat generation.

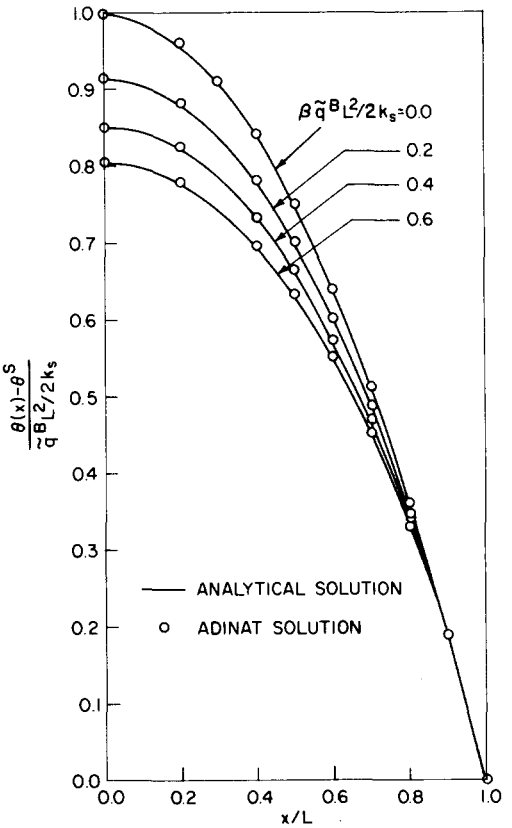

Fig. 2. Steady state temperatures of slab with internal heat generation and temperature dependent conductivity.

4.2. Transient temperature analysis of a slab subjected to simultaneous boundary convection and radiation

The slab shown in fig. 3 is initially at a uniform temperature θ_i. At time $t = 0^+$ the slab surfaces are exposed to convection (temperature $\theta_e = 0$, heat transfer coefficient h) and radiation (temperature $\theta_r = 0$, shape factor F, emissivity ϵ). The thermal conductivity k and heat capacity c are assumed constant.

In the analysis using ADINAT the Euler backward method was employed. The solution for θ^S (surface temperature) and θ^c (temperature at the center of the slab) depends upon two parameters, Bi and Γ. Figs. 4 and 5 show the temperature variations at the surface and at the center, respectively, for Bi = 0.2, 4, and for radiation parameters Γ of 0 and 4. The ADINAT solutions compare well with solutions obtained by Haji-Sheikh and Sparrow [17], who used a probability method.

In order to obtain the required accuracy in the ADINAT analysis the time step was changed during the response predictions. Table 4 summarizes the time step selections and gives the number of iterations used.

4.3. Transient temperature analysis of a solid cylinder subjected to simultaneous boundary convection and radiation

The solid cylinder shown in fig. 6 initially at a uniform high temperature θ_i is allowed to cool in air. The cylinder surface exchanges energy with the air by convection and radiation. The thermal conductivity k and heat capacity c of the cylinder are assumed constant. Since the cylinder is infinitely long, heat transfer takes place in the radial direction only.

The solution for θ^S (surface temperature) and θ^c (temperature at the center of the cylinder) depends upon three parameters, Bi, Γ and θ_e/θ_i. Figs. 7 and 8

Table 3
Summary of step-by-step integration

INITIAL CALCULATIONS

1. Form linear conductivity matrix $\mathbf{K}$, linear heat capacity matrix $\mathbf{C}$,
2. Initialize the following constants:
   tol $\leqslant 0.01$; nitem $\geqslant 3$;
   for $\alpha = 0$: $a_0 = 1/\Delta t$, $a_1 = 1$
   for $\alpha \neq 0$: $a_0 = 1/\alpha\Delta t$, $a_1 = 1/\alpha$
3. Calculate effective linear conductivity matrix:
   for $\alpha = 0$: $\hat{\mathbf{K}} = a_0\mathbf{C}$ and go to A
   for $\alpha \neq 0$: $\hat{\mathbf{K}} = \mathbf{K}^k + \mathbf{K}^c + a_0\mathbf{C}$
4. In linear analysis, triangularize $\hat{\mathbf{K}}$.

FOR EACH TIME STEP

A. In linear analysis, $\alpha \neq 0$

(i) Compute effective heat flow vector:

$$^{t+\alpha\Delta t}\hat{\mathbf{Q}} = {}^{t+\alpha\Delta t}\tilde{\mathbf{Q}} + {}^{t+\alpha\Delta t}\mathbf{Q}^e + a_0\mathbf{C}\,{}^t\boldsymbol{\theta}$$

(ii) Solve for nodal point temperatures at time $t + \Delta t$

$$\hat{\mathbf{K}}\,{}^{t+\alpha\Delta t}\boldsymbol{\theta} = {}^{t+\alpha\Delta t}\hat{\mathbf{Q}}$$

$$^{t+\Delta t}\boldsymbol{\theta} = a_1\,{}^{t+\alpha\Delta t}\boldsymbol{\theta} + (1 - a_1)\,{}^t\boldsymbol{\theta}$$

B. In linear and nonlinear analysis if $\alpha = 0$:

(i) If a new heat capacity matrix ($^t\mathbf{C}$) is to formed, update $\hat{\mathbf{K}}$ to obtain $^t\hat{\mathbf{K}}$,

$$^t\hat{\mathbf{K}} = a_0\,{}^t\mathbf{C}$$

(ii) Compute effective heat flow vector:

$$^t\hat{\mathbf{Q}} = {}^t\tilde{\mathbf{Q}} + {}^t\mathbf{Q}^c + {}^t\mathbf{Q}^r - {}^t\mathbf{Q}^k + a_0\,{}^t\mathbf{C}\,{}^t\boldsymbol{\theta}$$

(iii) Solve for nodal point temperatures at time $t + \Delta t$:

$$^t\hat{\mathbf{K}}\,{}^{t+\Delta t}\boldsymbol{\theta} = {}^t\hat{\mathbf{Q}}$$

C. In nonlinear analysis if $\alpha \neq 0$:

(i) If a new conductivity matrix ($^t\mathbf{K}^k$), nonlinear heat capacity matrix ($^t\mathbf{C}$), nonlinear convection matrix ($^t\mathbf{K}^c$), or radiation matrix ($^t\mathbf{K}^r$) is to be formed, update $\hat{\mathbf{K}}$ to obtain $^t\hat{\mathbf{K}}$ and factorize $^t\hat{\mathbf{K}}$,

$$^t\hat{\mathbf{K}} = {}^t\mathbf{K}^k + {}^t\mathbf{K}^c + {}^t\mathbf{K}^r + a_0\,{}^t\mathbf{C}$$

$$^t\hat{\mathbf{K}} = \mathbf{L}\,\mathbf{D}\,\mathbf{L}^T$$

(ii) Compute effective heat flow vector:

$$^{t+\alpha\Delta t}\hat{\mathbf{Q}} = {}^{t+\alpha\Delta t}\tilde{\mathbf{Q}} + {}^t\mathbf{Q}^c + {}^t\mathbf{Q}^r - {}^t\mathbf{Q}^k$$

(iii) Solve for increments in nodal point temperatures using latest $\mathbf{D}$, $\mathbf{L}$ factors:

$$\mathbf{L}\,\mathbf{D}\,\mathbf{L}^T\boldsymbol{\theta} = {}^{t+\alpha\Delta t}\hat{\mathbf{Q}}$$

(iv) If required iterate for heat flow equilibrium; then initialize

$$\boldsymbol{\theta}^{(0)} = \boldsymbol{\theta},\ i = 0$$

(a) $i = i + 1$

(b) Calculate $(i - 1)$st approximation to nodal point temperatures and time derivatives of nodal point temperatures:

$$^{t+\alpha\Delta t}\boldsymbol{\theta}^{(i-1)} = {}^t\boldsymbol{\theta} + \boldsymbol{\theta}^{(i-1)};$$

$$^{t+\alpha\Delta t}\dot{\boldsymbol{\theta}}^{(i-1)} = a_0({}^{t+\alpha\Delta t}\boldsymbol{\theta}^{(i-1)} - {}^t\boldsymbol{\theta})$$

(c) Calculate ith out-of-balance heat flow rates:

$$^{t+\alpha\Delta t}\hat{\mathbf{Q}}^{(i-1)} = {}^{t+\alpha\Delta t}\mathbf{Q}^{(i-1)} + {}^{t+\alpha\Delta t}\mathbf{Q}^{c(i-1)} + {}^{t+\alpha\Delta t}\mathbf{Q}^{r(i-1)} - {}^{t+\alpha\Delta t}\mathbf{Q}^{k(i-1)}$$

(d) Solve for ith correction to temperature increments:

$$\mathbf{L}\,\mathbf{D}\,\mathbf{L}^T\,\Delta\boldsymbol{\theta}^{(i)} = {}^{t+\alpha\Delta t}\hat{\mathbf{Q}}^{(i-1)}$$

(e) Calculate new temperature increments:

$$\boldsymbol{\theta}^{(i)} = \boldsymbol{\theta}^{(i-1)} + \Delta\boldsymbol{\theta}^{(i)}$$

(f) Iteration convergence if

$$\|\Delta\boldsymbol{\theta}^{(i)}\|_2 / \|^{t+\Delta t}\boldsymbol{\theta}\|_2 < \text{tol}$$

If convergence: $\boldsymbol{\theta} = \boldsymbol{\theta}^{(i)}$ and go to (v); If no convergence and $i <$ nitem: go to (a); otherwise restart using a new matrix reformation interval and/or a small time step size.

(v) Calculate new nodal point temperatures

$$^{t+\Delta t}\boldsymbol{\theta} = {}^t\boldsymbol{\theta} + a_1\boldsymbol{\theta}$$

show the temperature variations at the surface and at the center of the cylinder, respectively, for $1.0 \leqslant \mathrm{Bi} \leqslant 10$, $\Gamma = 1$, and $\theta_e/\theta_i = 0.55$.

In the figures the ADINAT solutions are compared with the finite difference solutions obtained by SUCEC and KUMAR [18] and good correspondence in the results is noted.

In this analysis the Euler backward method and trapezoidal rule have been used with the time step sizes summarized in table 5.

Some characteristics of the time integrations in a typical analysis of the problem are shown in fig. 9. It is seen that, using the Euler backward method, as the time step is decreased the predicted response converges uniformly to the response calculated with a very small time step, whereas, using the trapezoidal

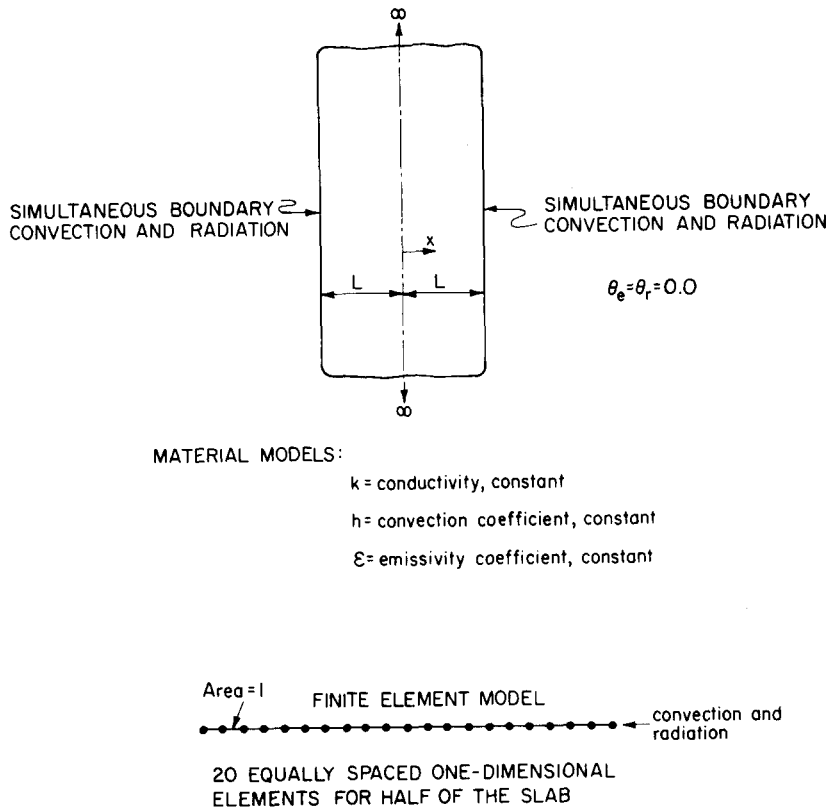

Fig. 3. Nonlinear temperature analysis of slab with radiation– convection boundary conditions.

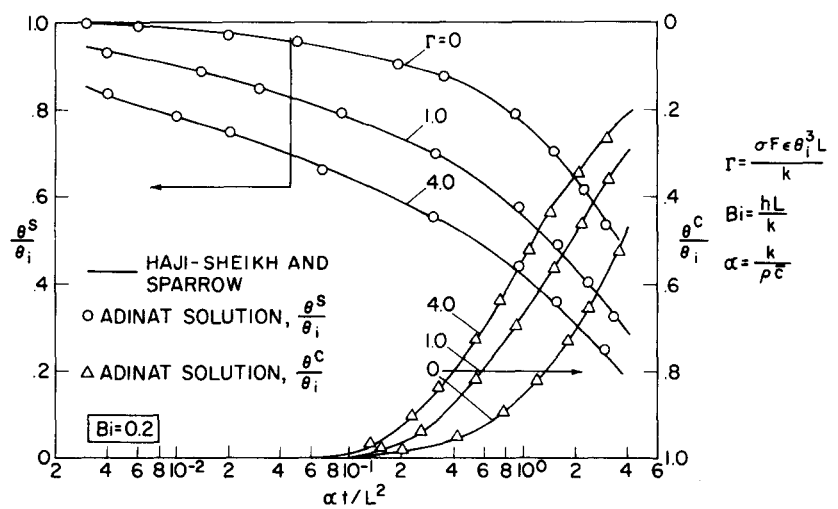

Fig. 4. Transient temperature results for a slab with radiation– convection boundary conditions, Bi = 0.2.

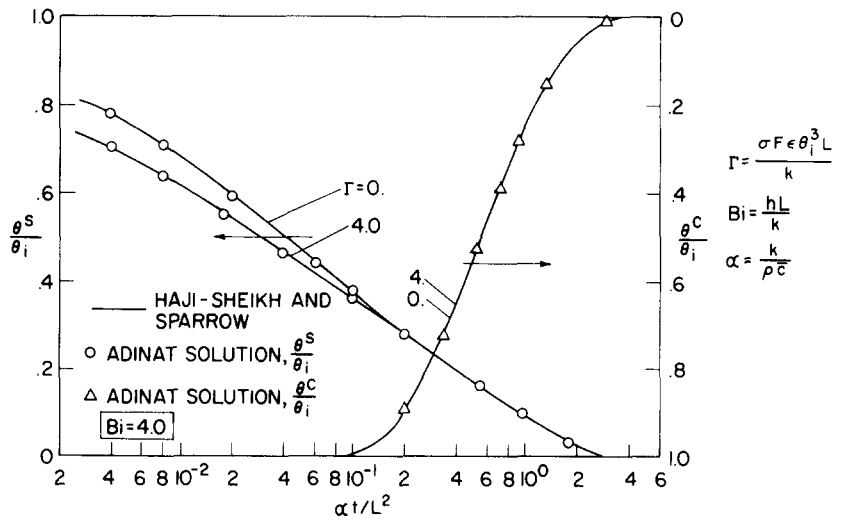

Fig. 5. Transient temperature results for a slab with radiation–convection boundary conditions, Bi = 4.0.

method with a large time step, the calculated response oscillates about the accurate solution.

4.4. Linear transient heat transfer analysis of a solid block subjected to convection cooling

The solid block in fig. 10 is initially at a uniform temperature 400°F. The block surfaces are suddenly exposed to convection conditions with a constant convection coefficient.

For the finite element analysis, 45 three-dimensional 8 node elements were used to model one quarter of the solid block. Fig. 11 gives the temperatures at points A and B (see fig. 10), as calculated using ADINAT and in an analytical solution [16]. Good correspondence between the results is observed.

In this analysis the trapezoidal rule has been used for the time integration and to obtain good solution accuracy, the time step was changed during the response predictions. Table 6 summarizes the time step selection and gives the solution accuracy (measured on the analytical solution).

Table 4
Transient analysis of a slab with radiation–convection boundary conditions

Shape factor $F = 1$ $L = 1$ in
emissivity $\epsilon = 1$ (black body) $\sigma = 0.118958 \times 10^{-10}$ Btu/in^2 · h · °R^4
thermal diffusivity $\alpha = 1$ in^2/h $k = 0.01$ Btu/in · h · °F
tol = 1×10^{-4}
Euler backward method used

Biot number	$t^* = \alpha t/L^2$	$\Delta t\alpha/L^2$	Number of time steps	average number of iterations
Bi = 0.2	$0 < t^* \leq 0.08$	0.002	40	3
$0 \leq \Gamma \leq 4$	$0.08 < t^* \leq 0.88$	0.02	40	2
	$0.88 < t^* \leq 3.88$	0.05	60	2
Bi = 4.0	$0 < t^* \leq 0.06$	0.001	60	3
$0 \leq \Gamma \leq 4$	$0.06 < t^* \leq 0.66$	0.01	60	2
	$0.66 < t^* \leq 3.66$	0.05	60	2

Table 5
Transient analysis of a solid cylinder with radiation–convection boundary conditions

Shape factor	$F = 1$	$\sigma = 0.118958 \times 10^{-10}$ Btu/in$^2 \cdot$ h $\cdot$ °R^4	
emissivity	$\epsilon = 1$ (black body)	$k = 0.5238$ Btu/in $\cdot$ h $\cdot$ °F	
thermal diffusivity	$\alpha = 1$ in^2/h	Trapezoidal integration rule (T.R.)	
Euler backward method (E.B.)		tol = 1×10^{-3}	

Biot number	$t^* = \alpha t/r_0^2$	$\Delta t\alpha/r_0^2$		Number of time steps		Average number of iterations	
		E.B.	T.R.	E.B.	T.R.	E.B.	T.R.
Bi = 10	$0 < t^* \leq 0.01$	0.0005	0.001	20	10	2	2
$\Gamma = 1$	$0.01 < t^* \leq 0.21$	0.005	0.01	40	20	2	2
$\theta_e/\theta_i = 0.55$	$0.21 < t^* \leq 1.21$	0.05	0.05	20	20	1	1
Bi = 2	$0 < t^* \leq 0.04$	0.002	0.004	20	10	2	2
$\Gamma = 1$	$0.04 < t^* \leq 0.44$	0.02	0.02	20	20	1	1
$\theta_e/\theta_i = 0.55$	$0.44 < t^* \leq 1.44$	0.1	0.1	10	10	1	1

5. Conclusions

A general and effective finite element solution scheme for the analysis of linear and nonlinear steady-state and transient heat transfer problems has been presented. Conduction, convection and radiation conditions are considered. The solution is achieved using isoparametric finite element discretization and direct time integration with a one step α-family integration scheme. This family includes the conditionally stable Euler forward method and the unconditionally stable Euler backward and trapezoidal methods. The solution procedures have been implemented and in the paper the results of various sample analyses are given. Based on the experience gained in the use of the solution techniques, it is concluded that the methods can be employed effectively to obtain accurate response predictions, but the nature of the transient heat transfer response may require a varying time step Δt in the analysis.

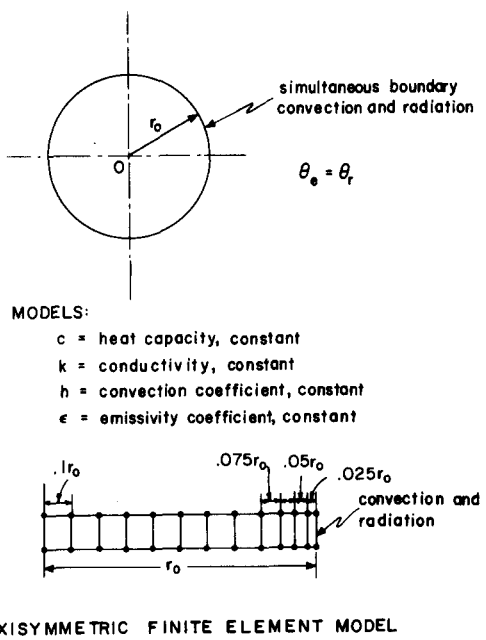

Fig. 6. Nonlinear temperature analysis of an infinite solid cylinder with radiation–convection boundary conditions.

Table 6
Transient analysis of a solid block with convection cooling (Using trapezoidal rule)

t (h)	Δt (h)	Number of time steps	Max. error measured on analytical solution (%)
$0 < t \leq 1$	0.1	10	5%
$1.0 < t \leq 7.0$	0.4	15	5%

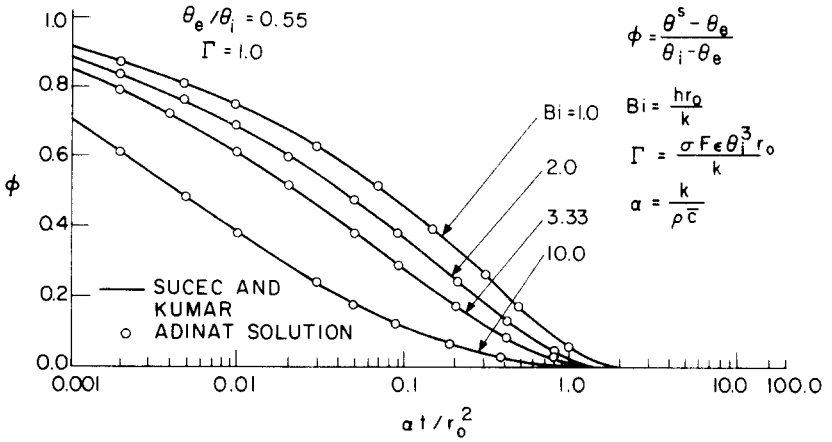

Fig. 7. Transient temperature distribution for solid cylinder subjected to simultaneous convection and radiation boundary conditions, at $r/r_0 = 1.0$.

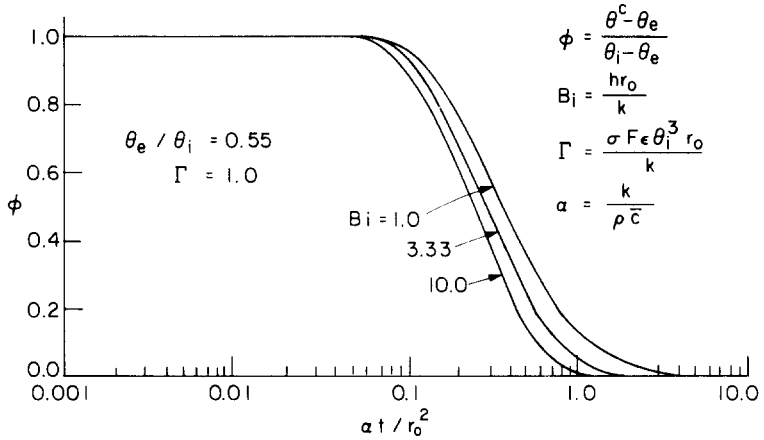

Fig. 8. Transient temperature distribution for solid cylinder subjected to simultaneous convection and radiation boundary conditions at $r/r_0 = 0.0$; ADINAT solution.

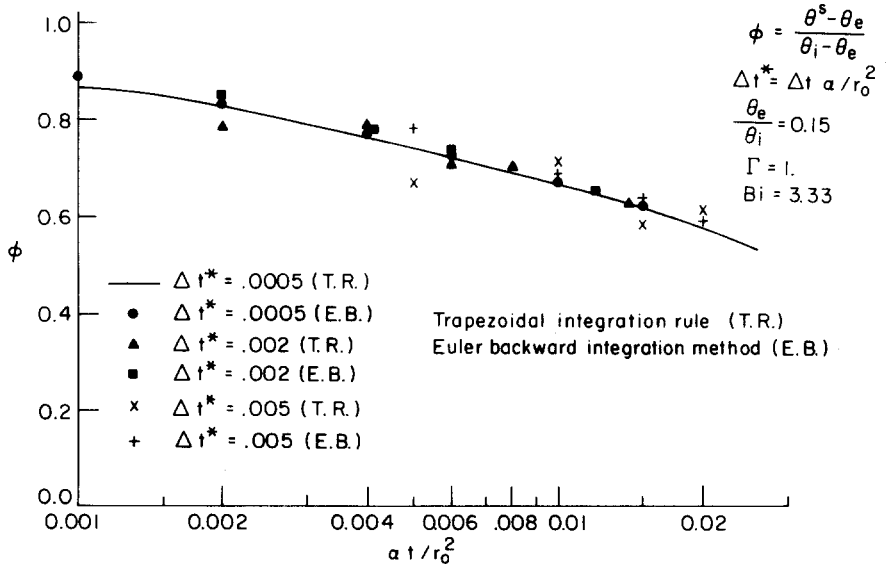

Fig. 9. Variation of surface temperature of solid cylinder subjected to simultaneous convection–radiation cooling.

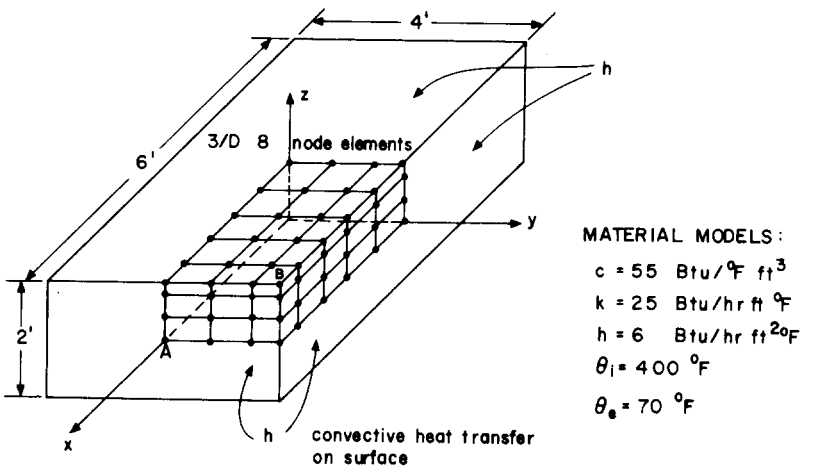

Fig. 10. Linear heat transfer analysis of a solid block subjected to convection cooling.

Considering the stability properties of the time integration scheme employed, the numerical experiences largely substantiated the conclusions of the theoretical stability analysis, although this analysis was based on the usual assumptions. Also, it is important to note, that no convergence difficulties in the solution of the nonlinear heat transfer equilibrium equations were encountered.

Acknowledgements

The work reported in this paper has been financed by the ADINA users group. We would like to acknowledge gratefully this support.

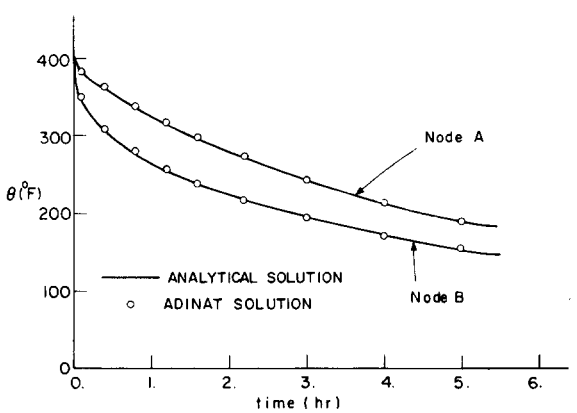

Fig. 11. Linear heat transfer analysis of a solid block subjected to convection cooling.

References

[1] O.C. Zienkiewicz, The Finite Element Method in Engineering Science (McGraw-Hill, London, 1971).
[2] K.J. Bathe and E.L. Wilson, Numerical Methods in Finite Element Analysis (Prentice-Hall, Englewood Cliffs, 1976).
[3] O.C. Zienkiewicz and Y.K. Cheung, The Engineer, Sept. 24, 1964.
[4] E.L. Wilson and R.E. Nickel, Nucl. Eng. Des. 4 (1966) 276.
[5] E.L. Wilson, K.J. Bathe and F.E. Peterson, Nucl. Eng. Design, 29 (1974) 240.
[6] M.A. Biot, J. Appl. Phys. 27 (1956) 240.
[7] K.J. Bathe, ADINAT-A Finite Element Program for Automatic Dynamic Incremental Nonlinear Analysis of Temperatures, AVL Rep. 82448-5, Mech. Eng. Dep. MIT (1977).
[8] L. Collatz, The Numerical Treatment of Differential Equations, (Springer-Verlag, New York, 1966).
[9] W.L. Wood, and R.W. Lewis, Int. J. Num. Meth. Eng. 9 (1975) 679.
[10] T.J.R. Hughes, Comp. Meth. Appl. Mech. Eng., 10 (1977) 135.
[11] A. Verruijt, Theory of Groundwater Flow (Gordon & Breach, New York, 1970).
[12] Y.C. Fung, A First Course in Continuum Mechanics (Prentice-Hall, London, 1969).
[13] S. Ramo, J.R. Whinnery and T. van Duzer, Fields and Waves in Communication Electronics (New York, 1965).
[14] K.J. Bathe and M.R. Khoshgoftaar, Int. J. Num. Anal. Meth. Geomech., to be published.
[15] R.O. Ritchie and K.J. Bathe, Int. J. Fracture, in press.
[16] V.S. Arpaci, Conduction Heat Transfer (Addison-Wesley, Reading, 1966).
[17] A. Haji-Sheikh and E.M. Sparrow, Trans. ASME. J. Heat Transfer, 89 (1967) 121.
[18] J. Sucec and A. Kumar, Int. J. Num. Methods Eng. 6 (1973) 297.